Journal of Hydrology 488 (2013) 84–100

Contents lists available at SciVerse ScienceDirect

Journal of Hydrology

journal homepage: www.elsevier.com/locate/jhydrol

Assessing future rainfall projections using multiple GCMs and a multi-site stochastic downscaling model

R. Mehrotra [a,*], Ashish Sharma [a], D. Nagesh Kumar [b], T.V. Reshmidevi [b]

[a] Water Research Centre, School of Civil and Env. Engineering, UNSW, 2052 Sydney, Australia
[b] Water Resources and Environmental Engineering, Department of Civil Engineering, Indian Institute of Science, Bangalore 560 012, India

ARTICLE INFO

Article history:
Received 27 March 2012
Received in revised form 6 November 2012
Accepted 23 February 2013
Available online 6 March 2013
This manuscript was handled by Konstantine P. Georgakakos, Editor-in-Chief, with the assistance of Ana P. Barros, Associate Editor

Keywords:
Climate change
Daily rainfall
Statistical downscaling
Multiple GCMs
Malaprabha catchment
Modified Markov model

SUMMARY

Impact of global warming on daily rainfall is examined using atmospheric variables from five General Circulation Models (GCMs) and a stochastic downscaling model. Daily rainfall at eleven raingauges over Malaprabha catchment of India and National Center for Environmental Prediction (NCEP) reanalysis data at grid points over the catchment for a continuous time period 1971–2000 (current climate) are used to calibrate the downscaling model. The downscaled rainfall simulations obtained using GCM atmospheric variables corresponding to the IPCC-SRES (Intergovernmental Panel for Climate Change – Special Report on Emission Scenarios) A2 emission scenario for the same period are used to validate the results. Following this, future downscaled rainfall projections are constructed and examined for two 20 year time slices viz. 2055 (i.e. 2046–2065) and 2090 (i.e. 2081–2100). The model results show reasonable skill in simulating the rainfall over the study region for the current climate. The downscaled rainfall projections indicate no significant changes in the rainfall regime in this catchment in the future. More specifically, 2% decrease by 2055 and 5% decrease by 2090 in monsoon (JJAS) rainfall compared to the current climate (1971–2000) under global warming conditions are noticed. Also, pre-monsoon (JFMAM) and post-monsoon (OND) rainfall is projected to increase respectively, by 2% in 2055 and 6% in 2090 and, 2% in 2055 and 12% in 2090, over the region. On annual basis slight decreases of 1% and 2% are noted for 2055 and 2090, respectively.

1. Introduction

The climate of India is dominated by monsoon and about 75–90% of the annual rainfall is received during four monsoon months, June–September. The Indian monsoon is one of the most dominant circulation systems and plays an important role in the general circulation of the atmosphere through the transport of heat and moisture from the tropics. More importantly, monsoon has great importance for the agrarian economy of India (Gadgil et al., 1999; Gadgil and Gadgil, 2006). Therefore, it is essential to understand the nature of climate change over regional India and its influence on different sectors like agriculture, human health, water resources, forestry, etc.

Several recent studies have focused on the possible influence of climate change on the Asian summer monsoon (Meehl and Arblaster, 2003; May, 2002; Solomon et al., 2007; Turner et al., 2007; Ashrit et al., 2003). Using a doubled CO_2 experiment data of the HadCM3 coupled model, Turner et al. (2007) observed 3.5% increase in the mean summer (JJAS) rainfall over the Indian land surface in the future. These increases mainly confined over north India, the southern peninsula and the Bay of Bengal. Using a transient green-house warming integration with the ECHAM4/OPYC3 CGCM, Hu et al. (2000) noted intensification of the Asian summer monsoon beyond 2030. Ashrit et al. (2003) used a CNRM ocean–atmosphere coupled model driven by changes in concentrations of greenhouse gases and sulphate aerosols and reported increased rainfall over northwest and far south regions during the second half of the 21st century. Krishna Kumar et al. (2011) examined the changes in the summer monsoon over India corresponding to the IPCC-SRES A1B emission scenarios. Three simulations from a 17-member Perturbed Physics Ensemble generated using Hadley Center Coupled Model (HadCM3) for the QUMP project, were used to drive PRECIS (Providing REgional Climates for Impact Studies). The results suggested 9–16% increase in the summer monsoon precipitation over India in 2080s compared to 1961–1990 period under global warming conditions. The fourth assessment report of the IPCC (2007) suggests no significant change in the Indian monsoon rainfall until about 2050s and about 8–10% increase towards the end of 21st Century. Also, projected future increase in the monsoon rainfall appears to be caused by an increase in the total moisture content in the

* Corresponding author. Tel.: +61 293855140; fax: +61 293856139.
E-mail addresses: Raj.mehrotra@unsw.edu.au (R. Mehrotra), a.sharma@unsw.edu.au (A. Sharma), nagesh@civil.iisc.ernet.in (D. Nagesh Kumar), reshmidevi@civil.iisc.ernet.in (T.V. Reshmidevi).

0022-1694/$ - see front matter Crown Copyright © 2013 Published by Elsevier B.V. All rights reserved.
http://dx.doi.org/10.1016/j.jhydrol.2013.02.046

atmosphere rather than an increase in the strength of monsoon circulation (IPCC, 2007; Stephenson et al., 2001). The report also suggests of an increase in the variability of monsoon rainfall from the current levels in the future; possibility of the stretching of monsoon season with an increase in the rainfall during May and October. However, the large inter-model differences in the simulation of Indian summer monsoon by the current GCMs and their low skill in representing the present-day Indian summer monsoon climate lead to lesser confidence in these projections. Meehl et al. (2007) examined June, July and August mean rainfall projections over the Indian region for 2080–2099 using the GCM rainfall projections for A1B emissions scenario and found that the inter-model spread of projections (noise) was larger than the mean rainfall increase (signal). Similarly, Meehl et al. (2008) reported a shift in seasonality (increasing the pre-monsoon at the expense of rainfall during summer if the effects of increasing black carbon and other aerosol forcings are considered. Hence there still remains considerable uncertainty among GCMs in mean projections of Indian monsoon rainfall.

Majority of the studies mentioned above deal with the assessment of climate change over India in the continental context, and as such provide very limited information on a local scale. Moreover, as GCMs provide only limited representation of topographical features, for example, the Himalayas in the north and Western Ghats along the west coast of India (Krishna Kumar et al., 2011); they fail to capture the dominant regional distribution of the monsoon rainfall patterns. Therefore, in order to understand the extent to which water balances in specific catchments will be affected in changed climate conditions, it is important to study the plausible changes in the frequency and magnitude of rainfall with a major focus on the regional distribution over localised catchments.

A diverse range of statistical and dynamical downscaling techniques have been developed and proposed in the literature to transfer the GCM output from coarse spatial scales to local or regional scales. In majority of statistical downscaling approaches, responses (precipitation/temperature) are either directly related to predictors (coarse scale atmospheric and local scale time-lagged variables), or to a discrete or continuous state, which is modelled as a function of the atmospheric and local scale predictors (Hewitson and Crane, 1996; Wilby and Wigley, 1997; Hughes et al., 1999; Charles et al., 2004; Stehlík and Bárdossy, 2002; Mehrotra and Sharma, 2005; Vrac and Naveau, 2007).

Till date we have come across only one study that deals with downscaling of rainfall to a catchment scale (Anandhi et al., 2008) across the Indian subcontinent. In this study, a Support Vector Machine (SVM) based model was used to downscale monthly rainfall over the Malaprabha catchment using the simulations from the third generation Canadian General Circulation Model (CGCM3) for SRES emission scenarios A1B, A2, B1 and COMMIT for the period 1971–2100. They reported substantial increase in annual rainfall in the future for almost all the scenarios considered.

This study attempts to examine the implications of climate change on the occurrence and distribution of daily rainfall over Malaprabha river catchment, India, which is considered to be a climatically sensitive region (Anandhi et al., 2008). A proper assessment of probable future rainfall and its temporal and spatial variability is necessary to study the impact of climate change on hydrology, water resources management, agriculture and floods over the study region. It may be noted that the statistical downscaling of multi-site daily rainfall using outputs of multiple GCMs is the first of its kind in India and therefore provides information useful to the researchers and professionals working in the water and agriculture sector.

The remainder of this paper is structured as follows. Section 2 presents an overview of downscaling model used in this study to translate information from GCM to local scale. Section 3 provides a description of the study region, data used and atmospheric predictor variables considered in the study. Section 4 presents the results and Section 5 provides a summary of the results and conclusions drawn from the study.

2. Downscaling model

The daily multi-site rainfall downscaling model (MMM-KDE) as described in Mehrotra and Sharma (2010) is used in this study. The MMM-KDE model has been used recently in many multisite daily rainfall generation as well as downscaling applications (for example, Mehrotra and Sharma, 2007b, 2010; Frost et al., 2011).

The model operates in two steps, first the simulation of rainfall occurrences (wet or dry days; a wet day is defined as a day with rainfall $\geqslant$0.3 mm) and simulation of rainfall amounts on the wet days, thereafter. In the following discussions rainfall occurrence at a location k and time t is defined as $Ro_t(k)$ and at the pth time step before the current as $Ro_{t-p}(k)$. The following describe in brief the rainfall occurrence and amount models, and the procedure that is used to incorporate the spatial dependence in the occurrence and amount simulations (Mehrotra and Sharma, 2010).

2.1. Rainfall occurrence downscaling model – MMM

The general structure of a rainfall occurrence downscaling model could be expressed as $Ro_t(k)|\mathbf{Z}_t(k)$, where $\mathbf{Z}_t(k)$ represents a vector of conditioning variables at a location k and at time t and can include previous time steps states (wet or dry) of rainfall to assign daily or short term persistence (Markovian dependence), atmospheric predictors to include influence of changing climate conditions and other variables to represent specific rainfall characteristics. If $\mathbf{Z}_t(k)$ contains $Ro_{t-1}(k)$ only then the model reduces to a simple Markov order one model whereas inclusion of variables representing higher time scale persistence also, would reduce it to a rainfall generator of Mehrotra and Sharma (2007b). Addition of atmospheric variables in the conditioning vector forms the Modified Markov Model (MMM) of Mehrotra and Sharma (2010).

Ignoring the site notations, the parameters of a stochastic model expressing the order one Markovian dependence are defined by $P(Ro_t|Ro_{t-1})$ with $\mathbf{Z}_t$ consisting of Ro_{t-1} only. Inclusion of additional continuous predictors $\mathbf{X}_t$ in the conditioning vector $\mathbf{Z}_t$ modifies the order one conditional dependence as $P(Ro_t|Ro_{t-1},\mathbf{X}_t)$. Expanding the conditional expression and rearranging the terms leads to the following:

$$P(Ro_t=1|Ro_{t-1}=i,\mathbf{X}_t) = \frac{P(Ro_t=1,Ro_{t-1}=i)}{P(Ro_{t-1}=i)} \times \frac{f(\mathbf{X}_t|Ro_t=1,Ro_{t-1}=i)}{f(\mathbf{X}_t|Ro_{t-1}=i)} \quad (1)$$

The first expression on the right of (1) defines the transition probabilities $P(Ro_t|Ro_{t-1})$ of a first order Markov model (representing order one dependence) whereas the second expression signifies the effect of inclusion of predictor set $\mathbf{X}_t$ in the conditioning vector $\mathbf{Z}_t$. As $\mathbf{X}_t$ usually consists of atmospheric variables and may also include the number of wet days in pre-specified aggregation time periods (as explained later), the second expression can be approximated as a multivariate normal which, when expanded, leads to the following simplification for $P(Ro_t|Ro_{t-1},\mathbf{X}_t)$:

$$P(Ro_t=1|Ro_{t-1}=i,\mathbf{X}_t) = P_{1,i} \times \frac{f(\mathbf{X}_t|Ro_t=1,Ro_{t-1}=i)}{[f(\mathbf{X}_t|Ro_t=1,Ro_{t-1}=i)P_{1,i}]+[f(\mathbf{X}_t|Ro_t=0,Ro_{t-1}=i)P_{0,i}]} \quad (2a)$$

$$= p_{1i}\frac{\frac{1}{\sqrt{\det(\mathbf{V}_{1,i})}}\exp\left\{-\frac{1}{2}(\mathbf{X}_t-\boldsymbol{\mu}_{1,i})\mathbf{V}_{1,i}^{-1}(\mathbf{X}_t-\boldsymbol{\mu}_{1,i})'\right\}}{\left[\frac{1}{\sqrt{\det(\mathbf{V}_{1,i})}}\exp\left\{-\frac{1}{2}(\mathbf{X}_t-\boldsymbol{\mu}_{1,i})\mathbf{V}_{1,i}^{-1}(\mathbf{X}_t-\boldsymbol{\mu}_{1,i})'\right\}p_{1i}\right]+\left[\frac{1}{\sqrt{\det(\mathbf{V}_{0,i})}}\exp\left\{-\frac{1}{2}(\mathbf{X}_t-\boldsymbol{\mu}_{0,i})\mathbf{V}_{0,i}^{-1}(\mathbf{X}_t-\boldsymbol{\mu}_{0,i})'\right\}p_{0i}\right]} \quad (2b)$$

where p_{1i} is the baseline transition probability of the first order Markov model defined by $P(Ro_t = 1|Ro_{t-1} = i)$ with p_{0i} being equal to $1 - p_{1i}$, $\boldsymbol{\mu}_{1,i}$ represents the mean vector $E(\mathbf{X}_t|Ro_t = 1, Ro_{t-1} = i)$ and $\mathbf{V}_{1,i}$ is the corresponding variance–covariance matrix. Similarly, $\boldsymbol{\mu}_{0,i}$ and $\mathbf{V}_{0,i}$ represent, respectively, the mean vector and the variance–covariance matrix of X when $(R_{t-1} = i)$ and $(R_t = 0)$ and det() represents the determinant operation.

Under specific instances where the assumption of a multivariate normal may not hold true, appropriate data transformation or use of appropriate distributions such as one described in Mehrotra and Sharma (2010) may be adopted.

In the present application, the vector $\mathbf{X}$ consists of variables representing aggregated wetness over the recent past and the selected atmospheric variables. Parameters of the MMM are estimated on a daily basis. The aggregated wetness over the recent past, $\mathbf{X}r_t$, is formulated as (following Harrold et al., 2003; Sharma and O'Neill, 2002; Mehrotra and Sharma, 2010):

$$\mathbf{X}r_t \in \{Xr_{j_1,t}, Xr_{j_2,t}, \ldots, Xr_{j_m,t}\}; \quad Xr_{j_i,t} = \frac{1}{j_i}\sum_{l=1}^{j_i} Ro_{t-l} \quad (3)$$

where m is the number of such predictors, Ro_{t-l} is the rainfall occurrence on the preceding lth day and $\mathbf{X}r_{j_i,t}$ describes how wet it has been over the preceding j_i days. The MMM is applied at each site in isolation and spatially correlated random numbers are used to reproduce the observed spatial dependence across the stations as discussed later.

2.2. Downscaling of rainfall amounts – KDE

The rainfall amount downscaling model is based on the kernel density estimation (KDE) procedure (Mehrotra and Sharma, 2007a,b, 2010). The model simulates rainfall amount for each day and at each location that the MMM occurrence downscaling model simulates as wet. The model is formulated to reproduce the temporal structure of the observed rainfall record in the simulations. On a given day, the model simulates rainfall at individual stations conditional on selected atmospheric variables as well as the previous day's rainfall. The observed spatial dependence across the stations is maintained by making use of spatially correlated random numbers. The use of rainfall amounts on the previous day as a conditioning variable imparts a Markov order one dependence to the downscaled series.

Similar to rainfall occurrences, the rainfall amount at time t and at station (k) is expressed as $R_t(k)$ and the associated conditioning vector as $\mathbf{X}_t(k)$. Dropping the site notation, k, the conditional kernel multivariate probability density for day t, $f(R_t|\mathbf{X}_t)$ for each site is defined as:

$$f(R_t|\mathbf{X}_t) = \sum_{i=1}^{N}\frac{1}{(2\pi\lambda^2 S')^{1/2}} w_i \exp\left(-\frac{(R_t - b_i)^2}{2\lambda^2 S'}\right) \quad (4)$$

where λ is a measure of spread of density around each data point, known as a kernel bandwidth, b_i is the conditional mean associated with each kernel, expressed as, $b_i = R_i - [\mathbf{S}_{XR}]^T[\mathbf{S}_{XX}]^{-1}\{[\mathbf{X}_t - \mathbf{X}_i]\boldsymbol{\psi}\}$ and S' is the measure of spread of the conditional density, estimated in terms of covariances of R and X series as, $S' = S_{RR} - \mathbf{S}_{XR}^T\mathbf{S}_{XX}^{-1}\mathbf{S}_{XR}$.The covariance of $[R_t, \mathbf{X}_t]$ is written as:

$$Cov[R_t, \mathbf{X}_t] = \begin{bmatrix} S_{RR} & \mathbf{S}_{XR}^T \\ \mathbf{S}_{XR} & \mathbf{S}_{XX} \end{bmatrix} \quad (5)$$

In Eq. (4), w_i is the weight associated with each kernel and represents the contribution of the kernel in forming the conditional probability density:

$$w_i = \frac{\exp\left(-\frac{1}{2\lambda^2}\{[\mathbf{X}_t - \mathbf{X}_i]\boldsymbol{\psi}\}^T[\mathbf{S}_{XX}]^{-1}\{[\mathbf{X}_t - \mathbf{X}_i]\boldsymbol{\psi}\}\right)}{\sum_{j=1}^{N}\exp\left(-\frac{1}{2\lambda^2}\{[\mathbf{X}_t - \mathbf{X}_j]\boldsymbol{\psi}\}^T[\mathbf{S}_{XX}]^{-1}\{[\mathbf{X}_t - \mathbf{X}_j]\boldsymbol{\psi}\}\right)} \quad (6)$$

The relative influence of each predictor in the conditional probability density is incorporated through $\boldsymbol{\psi}$ that represents a diagonal matrix of influence weights (Mehrotra and Sharma, 2007a). These influence weights can be calculated at the parameter estimation stage for each day using the observations of the moving window and multiple linear regression as described in Mehrotra and Sharma (2007b).

If the underlying probability density is Gaussian, the Gaussian reference bandwidth (Scott, 1992) may provide a reasonable estimate of the conditional probability density. However, the assumption of Gaussian distribution may not be appropriate for variables having skewed distributions, such as rainfall amounts. For these cases, varying the bandwidth with data points provides better estimate of the probability density more specifically at the lower boundary of the distribution. The local bandwidth, λ_{g_t} for each observation of $\mathbf{X}_t$ and R_t and at the tth data point of a given g series is written as:

$$\lambda g_t = \left(\frac{f(g_t)}{2\sqrt{\pi}f''(g_t)^2}\right)^{1/(q+4)} N^{(-1/(q+4))} \quad (7)$$

where $f(g_t)$ and $f''(g_t)$ respectively, are density and the second derivative of the density at data point t of the assumed distribution of g series, q is number of predictor variables and N is total number of observations. Assuming series g to be Gamma distributed, further simplification of (7) leads to the following:

$$\lambda g_t = \left(\frac{1}{2\sqrt{\pi}f(g_t)\left[\lambda^2 - \frac{2\lambda(\eta-1)}{g_t} + \frac{(\eta-1)(\eta-2)}{g_t^2}\right]^2}\right)^{1/(q+4)} N^{(-1/(q+4))} \quad (8)$$

where λ and η, respectively, are scale and shape parameters of the Gamma distribution. The derivation of Eq. (8) is discussed in Mehrotra and Sharma (2007b).

2.3. Modelling spatial dependences in rainfall occurrence and amounts

As discussed in the previous sections, stochastic downscaling of rainfall occurrences or amounts is carried out individually at each location. The spatial dependence in the downscaled simulations over many point locations is incorporated by using uniform random variates that are independent in time, but exhibit appropriate observed spatial dependence across the multiple point locations

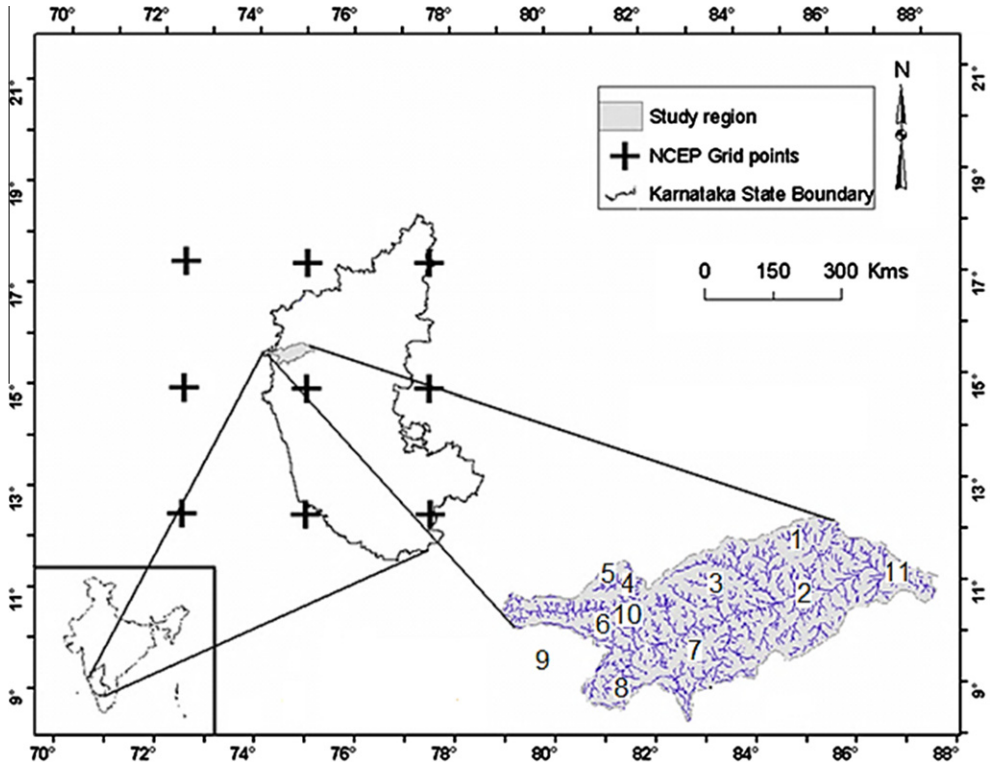

Fig. 1. Location of the Malaprabha river catchment in Karnataka, India. Raingauge station locations are shown in numbers with details provided in Table 1.

considered. For the case of S stations, let u_t be a vector of uniform [0,1] variates of length S at time step t. Our aim here is to define the vector $u_t\ (\equiv u_t(1), u_t(2), \ldots u_t(n_s))$ in such a way that for locations k and l, $corr[u_t(k), u_{t+1}(l)] = 0$ (or, random numbers are independent across time), but $corr[u_t(k), u_t(l)] \neq 0$ (or, random numbers are correlated across space). As a result, there is spatial dependence between individual elements of the vector u_t, this dependence is used to reproduce the observed spatial dependence across stations in the downscaled rainfall. More details on this rationale are available in Wilks (1998) and Mehrotra et al. (2006).

3. Datasets, study area and variables

This section presents the details on the data, study area and the selection of atmospheric variables.

3.1. Study area

The Malaprabha sub-basin lies in the extreme western part of the Krishna basin. It extends between 74°13′ and 75°10′E longitudes and 15°28′ and 15°55′N latitude in Belgaum district of Karnataka (Fig. 1). Malaprabha river originates from the Chorla Ghats (a section of the western Ghats) about 35 km south-west of Belgaum district in Karnataka, at an elevation of 792 m. The total catchment area is 2564 km^2. Malaprabha is one of the major tributaries of river Krishna (India) and the main source of water for irrigation in Belgaum, Dharwad, Bagalkot and Bijapur districts in Karnataka state. The Malaprabha catchment terrain is flat to gently undulating except for a few hillocks and valleys. The northern boundary is the common ridge between Malaprabha and Ghataprabha river catchments and the eastern ridge is separated between Malaprabha, Krishna and Tungabhadra river catchments. The southern and western boundaries are the common ridge between the Malaprabha and catchments of west flowing rivers.

3.2. Rainfall

For this study, a 30-year continuous record (from 1971 to 2000) of daily rainfall at 11 stations is used (Table 1). The climate of the

Table 1
Details of raingauge stations used in the study.

Index number	Station name	Station code	Elevation (m)	Latitude (°North)	Longitude (°East)	Average annual rainfall (mm)
1	Bailhongal TQ Off	30201	698	15.82447	74.86911	628
2	Belwadi	30204	690	15.71575	74.917	459
3	MK Hubli	30207	658	15.71783	74.70297	809
4	Desur	30304	750	15.74128	74.50242	1242
5	Zadshapur	30308	654	15.76375	74.49056	1174
6	Asoga	30702	670.5	15.62544	74.48325	1736
7	Bidi	30703	664	15.56539	74.65558	957
8	Gunji	30706	686	15.53772	74.49189	1476
9	Jamagaon	30707	692	15.55314	74.38194	3285
10	Khanapur	30710	668	15.63717	74.51075	1877
11	Soundatti SF	31003	658.8	15.75393	75.132	534

Table 2
Identified atmospheric predictors[a] on seasonal basis for occurrence and amount downscaling models.

Season	Rainfall occurrences	Rainfall amounts
JFMAM (January–May)	N–S gradient of MSLP	N–S gradient of GPH at 700 h Pa
	TD at 700 h Pa	MSLP
	N–S gradient of GPH at 700 h Pa	E–W gradient of SPH at 850 h Pa
	TD at 850 h Pa	N–S gradient of SPH at 500 h Pa
JJAS (June–September)	N–S gradient of MSLP	U-wind at 850 h Pa
	E–W gradient of MSLP	E–W gradient of MSLP
	TD at 500 h Pa	EPT at 850 h Pa
	TD at 700 h Pa	V-wind at 850 h Pa
OND (October–December)	TD at 500 h Pa	N–S gradient of SPH at 500 h Pa
	TD at 850 h Pa	SPH at 500 h Pa
	MSLP	
	N–S gradient of TD at 850 h Pa	

[a] TD: temperature depression (difference of air and dew-point temperatures), MSLP: mean sea level pressure; GPH: geopotential height; EPT: equivalent potential temperature; SPH: specific humidity.

Table 3
Observed and model simulated means and standard deviations of average number of wet days in a year and average annual rainfall over the study area for the current climate.

Conditioning variables	Number of wet days		Rainfall in mm	
	Mean	Standard deviation	Mean	Standard deviation
Observed	81	14	1289	415
Atmospheric variables only	83	10	1285	309
Atmospheric variables and previous 90 days wetness state	82	11	1282	325
Atmospheric variables and previous 180 days wetness state	83	12	1283	319
Atmospheric variables and previous 270 days wetness state	83	12	1289	326
Atmospheric variables and previous 365 days wetness state	84	13	1308	333

region is dominated by the monsoon and major part of the annual rainfall is received during four monsoon months, June–September. Recognising this and the fact that divergent rainfall generation mechanisms may prevalent during different parts of the year, more specifically in a changing climate, three seasons namely pre-monsoon (January–May, JFMAM), monsoon (June–September, JJAS) and post-monsoon (October–December, OND) are considered in this study. The study region shows considerable variation in spatial distribution of annual rainfall with upstream reaches (which is a part of the Western Ghats) recording more than 3000 mm, to around 400 mm near the Malaprabha reservoir. It receives an average annual rainfall of 1051 mm and the annual averages of maximum and minimum temperatures are 32 °C and 18 °C, respectively.

3.3. Large scale observed atmospheric variables

The required observed atmospheric variables at nine grid points over the study area are extracted from the National Center for Environmental Prediction (NCEP) reanalysis data provided by the NOAA-CIRES Climate Diagnostics Centre, Boulder, Colorado, USA, from their web site at http://www.cdc.noaa.gov/. These variables are available on 2.5° latitude × 2.5° longitude grids on a daily basis for the same period as the rainfall record (Fig. 1). As an observed rainfall value represents the total rainfall over a 24-h period ending at 0900 h (local time) in the morning, the available atmospheric measurements on the preceding day are considered as representative of today's rainfall.

3.4. Large scale GCM variables

The World Climate Research Programme's Coupled Model Intercomparison Project phase 3 (CMIP3) multimodel dataset contains results from more than 20 major global climate models developed around the world (Meehl et al., 2007). This information has been widely utilised for climate research and prediction. Although GCMs are capable of reproducing the many important aspects of the current climate at regional and continental scales including the changes in the patterns of different climate variables over time, their predictive skill varies considerably from model to model and over regions of interest. Thus, climate scientists often use multi-model information as a method for dealing with inter-model variability in future projections (Fordham et al., 2012; Pierce et al., 2009).

The limited data availability of the required daily atmospheric variables at the CMIP3 archive controlled the selection of five GCMs for the present study. These include: (a) Bjerknes Centre for Climate Research (BCCR), Univ. of Bergen, Norway, BCCR-BCM2.0; (b) Meteorological Research Institute (MRI), Japan, MRI-CGCM2; (c) Commonwealth Scientific and Industrial Research Organisation (CSIRO), Australia, CSIRO-mk3.5; (d) Max Planck Institute for Meteorology (MPI), Germany, MPI-ECHAM5; and (e) Institute Pierre Simon Laplace (IPSL), France, IPSL-CM4.

GCM datasets of atmospheric variables for the baseline period (covering a 30-year period between 1971 and 2000 and representing the current climate) and the future climates by 2055 (2046–2065) and 2090 (2081–2100) periods are considered in the analysis. Again, the selection of future time slices is limited by the data availability for these time periods. These variables are extracted from a single continuous (transient) run (corresponding to A2 SRES emission scenarios) for the grid nodes over the study region. The A2 scenario is at the higher end of the SRES emissions scenarios (but not the highest), and this is preferred because a low emissions scenario potentially provides less information from an impacts and adaptation point of view. In addition, the current trajectory of emissions (1990 to present) corresponds to a relatively high emissions scenario similar to A2. As an observed rainfall value represents the total rainfall over a 24-h period ending at 0900 h (local time) in the morning, similar to the reanalysis data, the available atmospheric measurements on the preceding day are considered as representative of today's rainfall.

Since the resolution of GCMs varies, output of each GCM is interpolated back onto the nine NCEP grids (2.5° latitude by 2.5° longitude). For defining a grid averaged value and north–south and east–west gradients, all nine grid point values are used to smoothen out the bias and spatial shifts, if any, at an individual grid point values.

3.5. Adjustment of GCM data

Limitations and assumptions in the modelling of the energy and moisture cycles and, the simulation of clouds in GCMs contribute significant uncertainties in GCM outputs (Solomon et al., 2007). Because of these limitations, a GCM may not simulate climate variables accurately and there is a difference between the

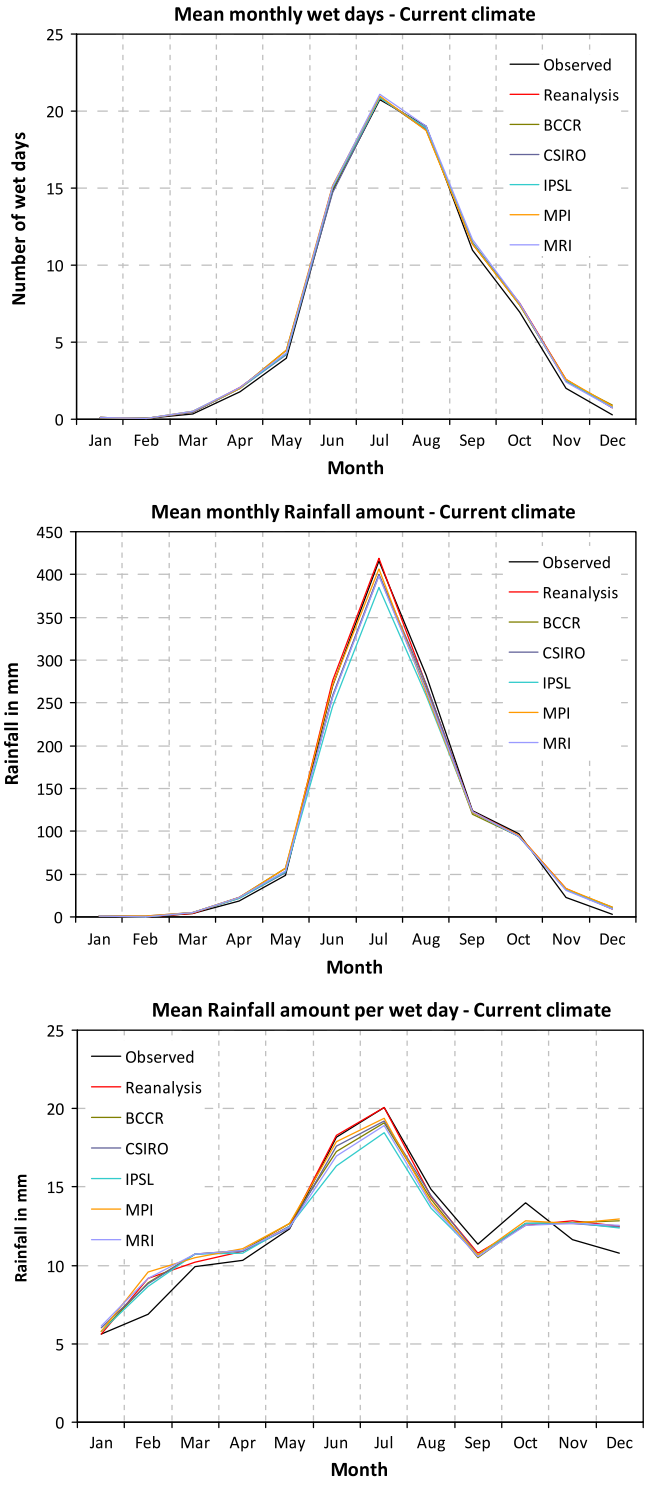

Fig. 2. Observed and model simulated monthly wet days, rainfall amounts and per wet day rainfall in a month for the current climate (1971–2000) over the study area.

observations and simulations, known as bias and this limits the direct application of GCM simulations in downscaling and hydrological modelling studies.

An examination of the means and standard deviations of current climate GCM and corresponding reanalysis atmospheric fields (1971–2000) at daily, monthly, seasonal and annual time scales suggest subtle differences in these characteristics. This requires some scaling correction to be carried out on the GCM data before use in the downscaling application. The GCM overall climatological mean bias over the future period includes GCM systematic bias (as observed for the current climate) and the climate change shift (from the current to the future). We aim to correct the former one in the bias correction approach under the assumption that the bias is stationary i.e. does not change with time and does not affect the overall climate dynamics.

We adjust the GCM data for the baseline (1971–2000) and future climate periods (2046–2065 and 2081–2100) by adopting a nested bias correction (NBC) procedure (Johnson and Sharma, 2012). In the approach, the GCM series (current and future climates) is corrected for biases in the mean, standard deviation and LAG 1 auto-correlation at daily, monthly, seasonal and annual time scales simultaneously by ensuring that systematic biases in the GCM atmospheric fields are removed before their use for downscaling while the mean shift from current to future climate is maintained.

Sharma et al. (in press) and Johnson and Sharma (2011) have shown that the use of NBC for bias correction of atmospheric variables helps reproducing the observed low frequency variability in the rainfall simulations, and offers a better representation than the use of alternative bias formulations such as quantile correction. When the intent is to simulate the "sustained extremes" that are of considerable importance in water resources planning and design, the use of such an approach leads to improved results. Daily means and standard deviations for the standardization procedure are estimated by considering a moving window of 31 days centred on the current day.

3.6. Identification of significant predictors

Atmospheric circulation and moisture strongly influence the monsoon climate. Sea level pressure (SLP), geo-potential height, air temperature, wind speed and other variables have been used to define atmospheric circulation (e.g. Harpham and Wilby, 2005; Buishand et al., 2004; Charles et al., 1999). A warmer climate is expected to accelerate evaporation and release more moisture in the atmosphere, leading to higher rainfall rates and greater intervals between rain events (Trenberth et al., 2003). Different forms of atmospheric moisture have been used by the researchers in the past (Crane and Hewitson, 1998; Cavazos, 1999; Charles et al., 1999; Easterling, 1999; Harpham and Wilby, 2005; Buishand et al., 2004; Evans et al., 2004). It may be noted that the absolute form of moisture such as relative humidity does not really carry the 'true climate signal' as a warmer climate can hold more moisture and therefore additional information about temperature is needed to know the amount of moisture that can precipitate in a warmer climate. Following this, Charles et al. (1999) suggest using difference of air and dew point temperatures whereas Evans et al. (2004) advocate using equivalent potential temperature as one of the predictors. On the basis of the results of earlier downscaling studies, we pick a large set of atmospheric predictors comprising of circulation and moisture variables at various levels and their horizontal and vertical gradients, as the potential predictors. A nonparametric stepwise predictor identification analysis is carried out at daily time scale to identify sets of significant atmospheric predictors for each season and for occurrence and amounts models. A partial correlation analysis is carried out at each time step to analyse the predictive capability of the additional variable being included. As some of these predictors might be highly correlated among themselves, at each stage of predictor identification exercise, a screening is carried out to see whether identified predictor at current stage is highly correlated with predictors picked up at previous stages (predictors having absolute linear correlation higher than 0.85 are ignored). To account for the short term persistence in the rainfall downscaling process, previous day rainfall is in-

Table 4
Observed and model simulated seasonal and annual means and standard deviations of wet days and rainfall totals over the study area for current climate (1971–2000).

Data set/season	Wet days				Rainfall amount			
	Pre-monsoon	Monsoon	Post-monsoon	Annual	Pre-monsoon	Monsoon	Post-monsoon	Annual
Means								
Observed	6.3	65.6	9.2	81.1	72.1	1093.1	123.7	1288.8
Reanalysis	6.9	66.2	10.9	84.0	80.9	1090.0	137.4	1308.3
BCCR	7.1	66.0	10.8	84.0	85.0	1043.5	137.2	1265.7
MRI	7.1	66.9	10.7	84.7	83.0	1042.6	134.3	1259.9
CSIRO	6.9	65.9	10.7	83.5	80.6	1053.9	135.9	1270.3
MPI	7.2	66.3	10.9	84.3	85.3	1062.0	139.3	1286.7
IPSL	6.9	66.3	10.7	83.9	81.3	1010.7	135.8	1227.8
Standard deviations								
Observed	2.4	6.6	3.3	7.7	29.2	280.3	58.7	289.1
Reanalysis	2.3	7.7	3.1	9.0	32.1	240.9	49.2	249.4
BCCR	2.3	7.3	3.3	8.7	35.1	226.1	52.2	238.2
MRI	2.3	6.1	3.2	8.2	32.9	205.0	49.3	219.2
CSIRO	2.4	7.5	3.6	9.9	35.1	240.5	55.5	263.4
MPI	2.5	7.6	3.8	9.8	37.6	235.1	57.6	254.8
IPSL	2.2	7.5	2.8	9.2	31.8	219.2	44.9	235.6

cluded as a pre-identified predictor in the conditioning vector for each season before carrying out the predictor identification exercise. For rainfall occurrences, one additional pre-identified predictor, namely, previous 365 days area averaged wetness state is also included. Table 2 provides a list of atmospheric predictors identified as significant for occurrence and amount processes for all the seasons.

4. Application of downscaling model and discussion of results

For the rainfall occurrence downscaling model (MMM), we consider individual at-site Markov order one models conditional on pre-identified atmospheric variables (common across all stations) and previous 365 days (at individual station) wetness state. The 365 days wetness state predictor is identified based on a sensitivity analysis. The analysis is performed using current climate data and varying the aggregated wetness state from 90 days to 365 days with 30 days interval. As shown in Table 3, the 365 days aggregated wetness state predictor is found to provide better representation of the observed standard deviation of annual number of wet days and rainfall amount in the current climate simulations. Thus, the short term persistence in the downscaled rainfall is maintained through order one Markovian structure, while long-term persistence is introduced through previous 365 days wetness state and nested bias corrected atmospheric variables. Nonzero precipitation amounts are downscaled conditional on atmospheric variables and previous day's rainfall, for each day and station, defined as wet by the MMM occurrence downscaling model. The inter-station spatial correlations in downscaled occurrence and amounts are induced through spatially correlated random numbers as discussed in Section 3.2.

The model is calibrated using observed rainfall and reanalysis data for the time period (1971–2000) and is evaluated using the GCM data for the same time period. The calibrated model is run for two 20 years time windows (2046–2065 and 2080–2100) to obtain rainfall predictions around 2055 and 2090, respectively.

4.1. Results

A range of spatial and temporal characteristics of observed and model simulated rainfall on daily, monthly, seasonal and annual basis are calculated, compared and evaluated to assess the performance of downscaling model for the current climate and, to examine the impact of changed climate on rainfall in the future. The statistics of downscaled rainfall time series are derived from 100 realisations and the median value is used to compare the results. Results of spatial correlations, average number of wet days and rainfall amounts are presented for all stations whereas for some statistics catchment area averaged values are presented. The year to year distributional behaviour of the observed and simulated series of rainfall occurrence and amounts is analysed at individual locations and, presented and discussed at two representative stations.

First, results of model calibration and verification for the current climate are presented and discussed. This is followed by the presentation and discussion of changes in few important rainfall statistics in years 2055 and 2090.

4.2. Model results for the current climate

4.2.1. Average rainfall statistics

For downscaling applications planned for use in agriculture, reservoir operation and flood management strategies, accurate simulation of the number of wet days and rainfall amounts assume significance. Fig. 2 presents the plots of area averaged observed and model simulated median values of number of wet days (top plot) and rainfall amounts (middle plot) and, amount per wet day (bottom plot) in each month for model calibration (using reanalysis data) and evaluation (using GCM data) phases. As can be seen from these plots, the model provides a good fit to the monthly number of wet days and rainfall amount for calibration and evaluation phases for all months. A slight underestimation of rainfall amounts for July month by the IPSL model is noted. The amount per wet day is over simulated by all the models during December and pre-monsoon period and under simulated during monsoon period.

Similar to Fig. 2, Table 4 presents the seasonal and annual means and standard deviations of observed and model simulated number of wet days and rainfall amounts averaged over the study area. In general, reanalysis and GCM data based simulations oversimulate the mean number of wet days and rainfall amount during pre-monsoon and post-monsoon seasons and under-simulate the standard deviation of rainfall amount during monsoon season. However, these differences are minor and overall performance of the downscaling model for calibration and evaluation phases at monthly, seasonal and annual level is deemed satisfactory.

Scatter plots of observed and model simulated median values of annual number of wet days, annual rainfall and amount per wet day at individual stations are presented in Fig. 3. In these plots, observed statistics is plotted on the horizontal while simulated one is

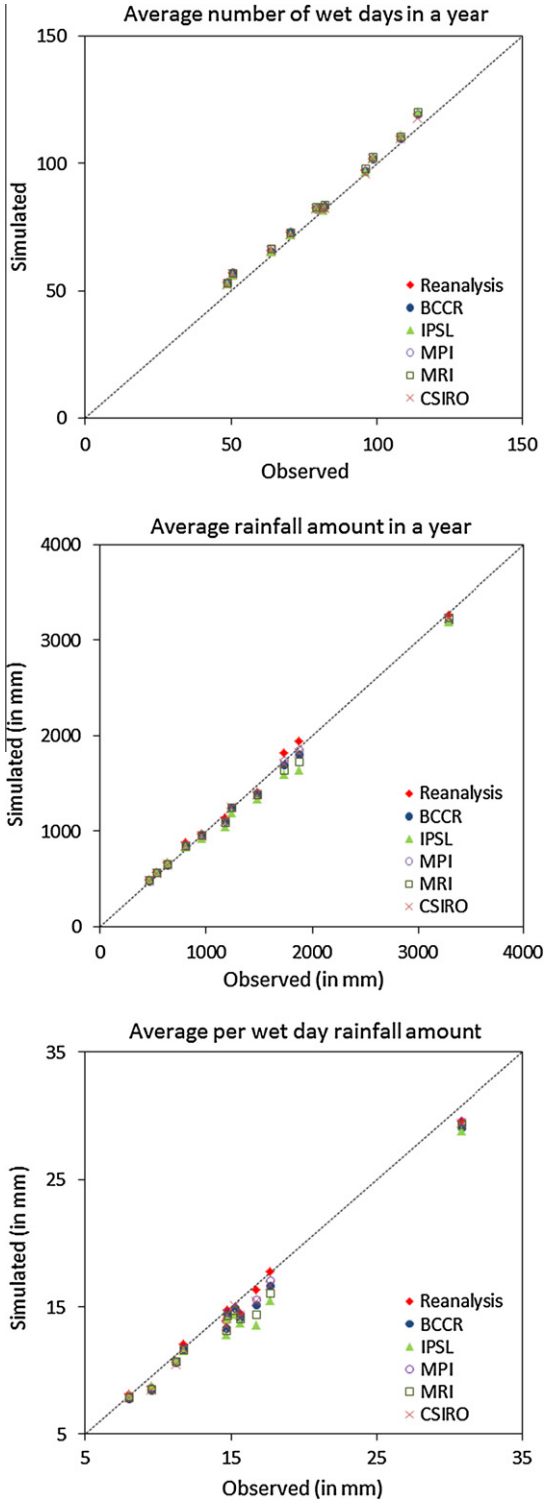

Fig. 3. Observed and model simulated annual wet days, rainfall amounts and per wet day rainfall in a year for the current climate (1971–2000) over the study area. Symbols on the graphs indicate stations.

shown on the vertical axis. Filled circles on these plots represent stations with colors used to differentiate amongst the GCM data sets used to derive these statistics. In general, all GCMs simulate similar annual number of wet days and rainfall amounts (top and middle plots) at all stations with IPSL and MRI models slightly under simulating rainfall at a few locations. These differences are more pronounced in the bottom plot where scatter plot of amount per wet day is shown. The stations with noticeable differences are located in the upper forested region of the catchment which is a part of the Western Ghats. Although, the model grid resolution, proximity to the coast, land use and representation of topography in the model might have some bearing on the results, the exact reason behind such differences is quite complex and requires further investigation.

4.2.2. Distribution of average annual wet days and rainfall amounts

Proper simulation of year-to-year distribution of annual number of wet days and rainfall amount in the downscaled series is important for efficient design and management of water resource projects. Fig. 4 compares the distribution plots of number of wet days in a year and annual rainfall amounts of the observed and downscaled rainfall series for two representative stations (Bailhongal and Asoga with index number 1 and 6 of Table 1, respectively). The top row shows the distribution of annual number of wet days, middle annual rainfall while the bottom row presents the distribution of average rainfall amount per wet day in a year. In general, the performance of the downscaling model in reproducing the year-to-year distribution of observed (black) number of wet days in a year and annual rainfall amounts using reanalysis (red) and GCMs data (other colors) at both stations is satisfactory (first two rows). The year-to-year distribution of amount per wet day is simulated reasonably well by the model using reanalysis data at both stations while GCM data derived results show under simulation of this statistic for low exceedance probabilities at Asoga stations (bottom row). These differences are more pronounced for IPSL and MRI data derived results. It may be noted that Asoga is located in the upper forested part of the catchment while Bailhongal is located in the lower region with flat topography (Fig. 1). It appears that GCMs have limitations in simulating the climate in the Western Ghats region. Similar results are obtained for other stations as well and are not presented here for the space limitation.

4.2.3. Number of wet and dry spells and daily maximum rainfall

Continuous wet and dry spells, and daily rainfall peaks form the basis of reservoir design and operation, flood estimation and agricultural studies. Therefore, proper simulation of these rainfall characteristics is of significance in catchment studies. Table 5 presents the statistics of observed and models simulated average number of wet and dry spells of varying durations, associated rainfall in wet spells and number of days with heavy rainfall (3rd percentile daily rainfall). Wet and dry spells of shorter durations are, in general, oversimulated while rainfall amount in longer duration wet spells is under simulated by all the models. Other statistics including number of days with heavy rainfall are reasonably well simulated by all the models.

Similar to Table 5, the first column of Fig. 5 compares the observed and model simulated maximum daily rainfall while the second and third columns present the average occurrences of wet spells of 5–7 days and >7 days in a year and associated average rainfall in these wet spells at all stations. Finally, the last column presents the average occurrences of dry spells of 9–18 and >18 days in a year. In these plots observed statistics is shown on the horizontal while simulated one is shown on the vertical axis and symbols are shown for individual stations. For a perfect match, all symbols should align along the diagonal dotted line. The downscaled simulations from all the GCMs largely reproduce these rainfall attributes at all stations albeit some scatter for average number of wet and dry spells. In general, the wet spells of 5–7 days and dry spells of greater than 18 days are over simulated at all stations by all the models. Average rainfall in the wet spells is reasonably well simulated with the exception of under simulation at Jamagaon station (index number 9) which receives substantial amount of annual rainfall (Table 1) and is located in the upper region of the

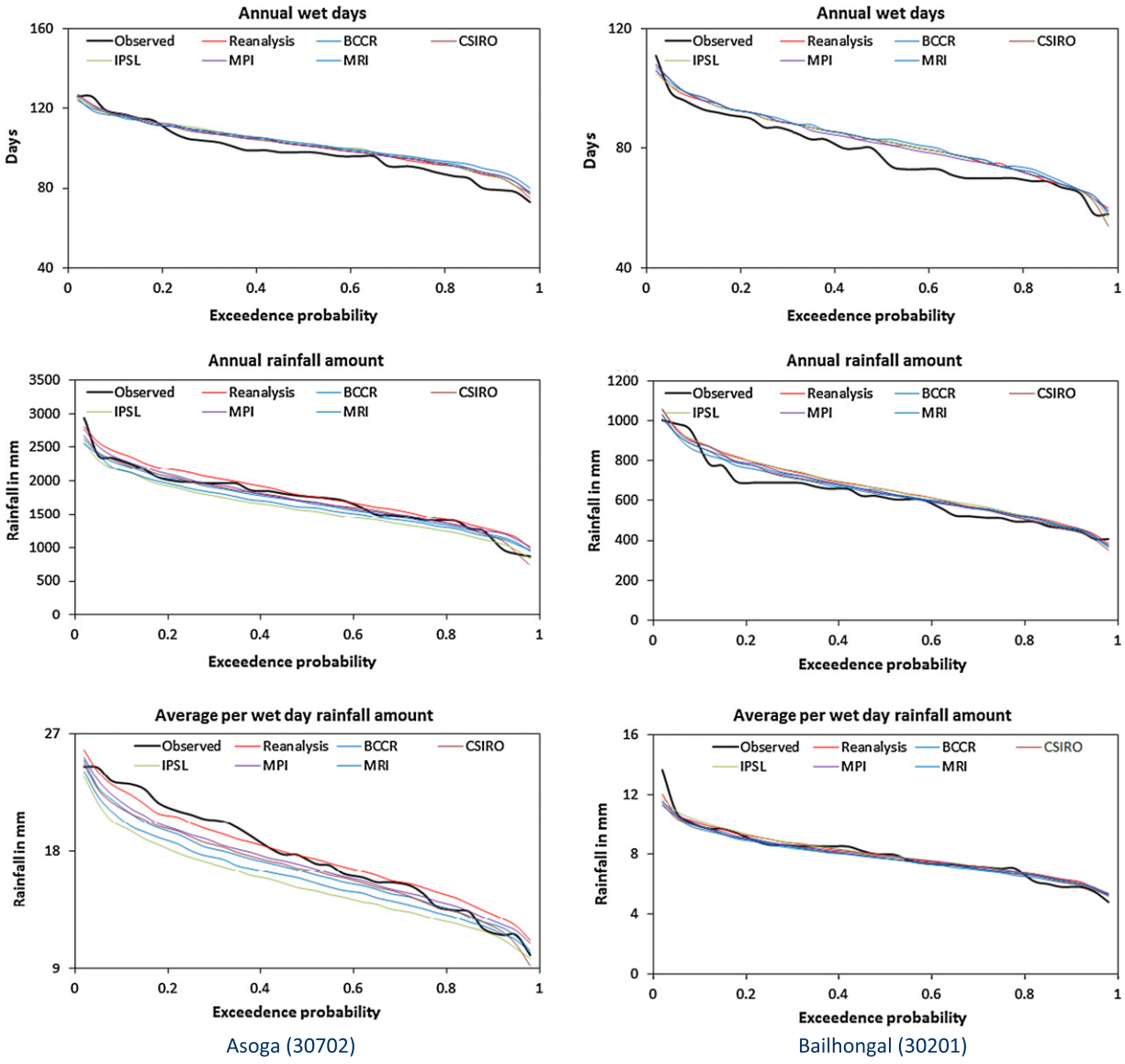

Fig. 4. Year to year distribution of observed and model simulated (median values) annual wet days and rainfall totals for current climate (1971–2000) at two representative stations, Asoga (30702) and Bailhongal (30201).

catchment which is a part of the Western Ghats (Table 1 and Fig. 1).

4.2.4. Spatial dependence of rainfall

A log-odds ratio provides a measure of evaluation of the spatial dependence of binary rainfall across stations (Edwards, 1963). Similarly, cross correlation provides a measure of spatial dependence of continuous time series such as aggregated number of wet days or rainfall amounts at a station pair. Accurate reproduction of spatial correlation of rainfall is often necessary to evaluate the hydrological or agricultural behaviour of a region and can influence significantly the discharge of a river and the formation

Table 5
Observed and models simulated extreme rainfall characteristics for current climate (1971–2000).

Statistics/model	Observed	Reanalysis	BCCR	MRI	CSIRO	MPI	IPSL
No of dry spells of 2–9 days (nos.)	11.3	13.7	14.0	13.8	13.6	13.6	13.9
No dry spells of 10–18 days (nos.)	2.5	2.6	2.7	2.6	2.7	2.6	2.6
No of dry spells of >18 days (nos.)	2.2	2.6	2.6	2.6	2.5	2.6	2.6
No of wet spells of 2–4 days (nos.)	7.5	9.0	9.3	9.1	9.0	9.0	9.2
No of wet spells of 5–7 days (nos.)	1.7	2.1	2.2	2.2	2.1	2.1	2.1
No of wet spells of >7 days (nos.)	2.2	2.2	2.1	2.2	2.2	2.3	2.2
Average rainfall in wet spells of 2–4 days (mm)	28.7	27.8	28.0	28.1	27.8	28.2	28.3
Average rainfall in wet spells of 5–7 days (mm)	69.1	68.3	67.6	67.4	67.6	68.4	67.0
Average rainfall in wet spells of >7 days (mm)	309	275	259	248	268	260	246
No of days with heavy rainfall (nos.)	24.7	25.4	24.6	24.4	24.7	25.0	23.8

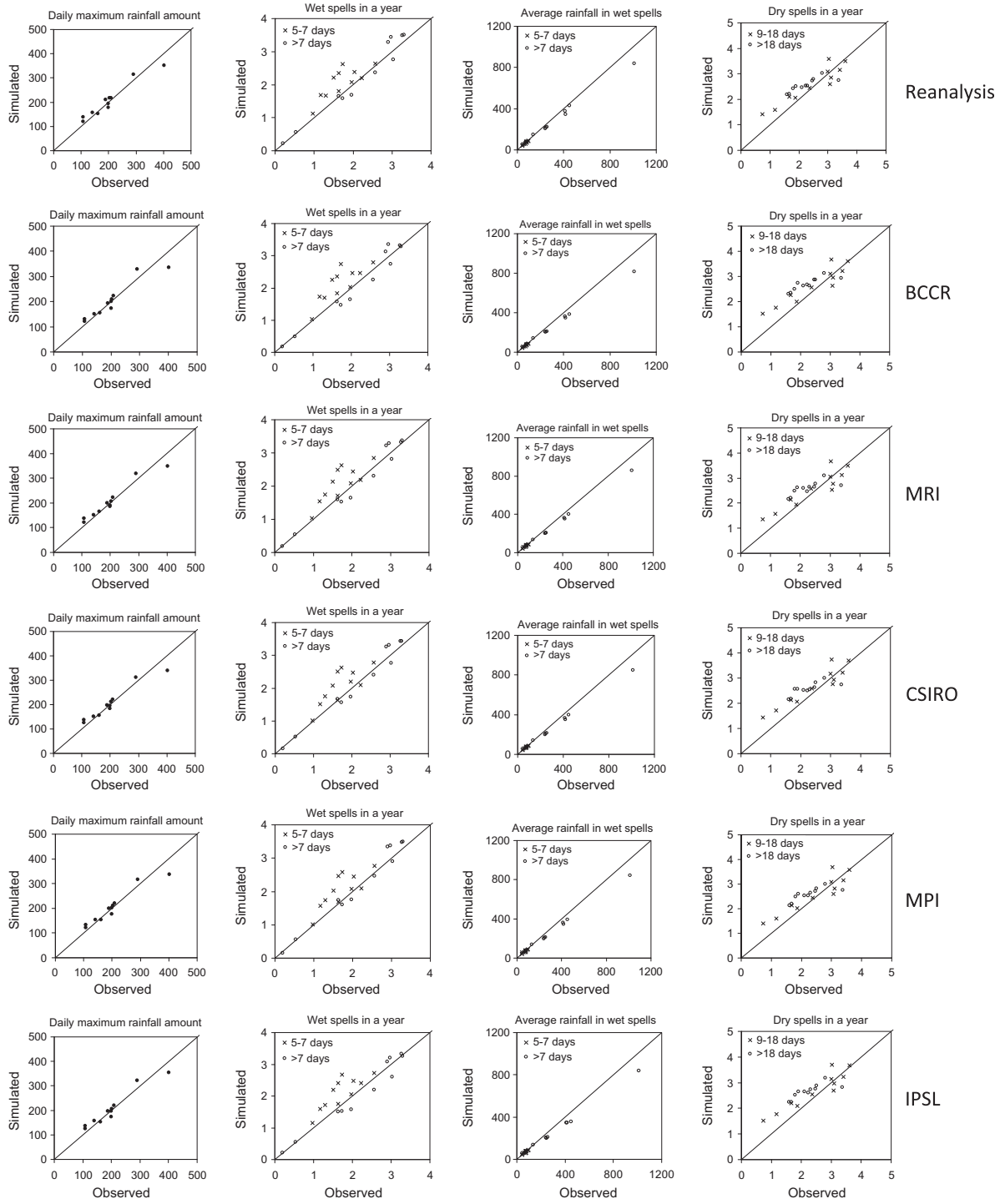

Fig. 5. Scatter plots of observed and model simulated daily maximum rainfall amount, average number of dry and wet spells of different durations in a year and average rainfall amounts in wet spells for current (1971–2000) climate for all stations. Symbols on the graphs indicate stations.

of floods. The first column of Fig. 6 presents the scatter plots of observed and model simulated daily log-odds ratios while the second column compares the cross correlations of aggregated annual wet days at all stations for the current climate. Similarly, the scatter plots of daily and annual rainfall amounts are shown in columns 3 and 4 of Fig. 6, respectively. Each point on these plots indicates the log-odds ratio/cross correlation evaluated for a pair of raingauge stations with observed statistic plotted on the horizontal and simulated one on the vertical axis. The model accurately reproduces the daily dependence between the stations, however, shows a large scatter for the spatial dependence at annual level. It appears that the current structure of spatial dependence adopted in the downscaling model is insufficient to capture the observed higher time scale spatial dependence in the simulations and requires some refinements. This limitation can influence the results of the studies where aggregated rainfall is used.

4.3. Model results for years 2055 and 2090

The changes in rainfall in the future climates are compared against the current climate GCM median estimate. This is adopted to cancel the biases introduced in some statistics as a result of

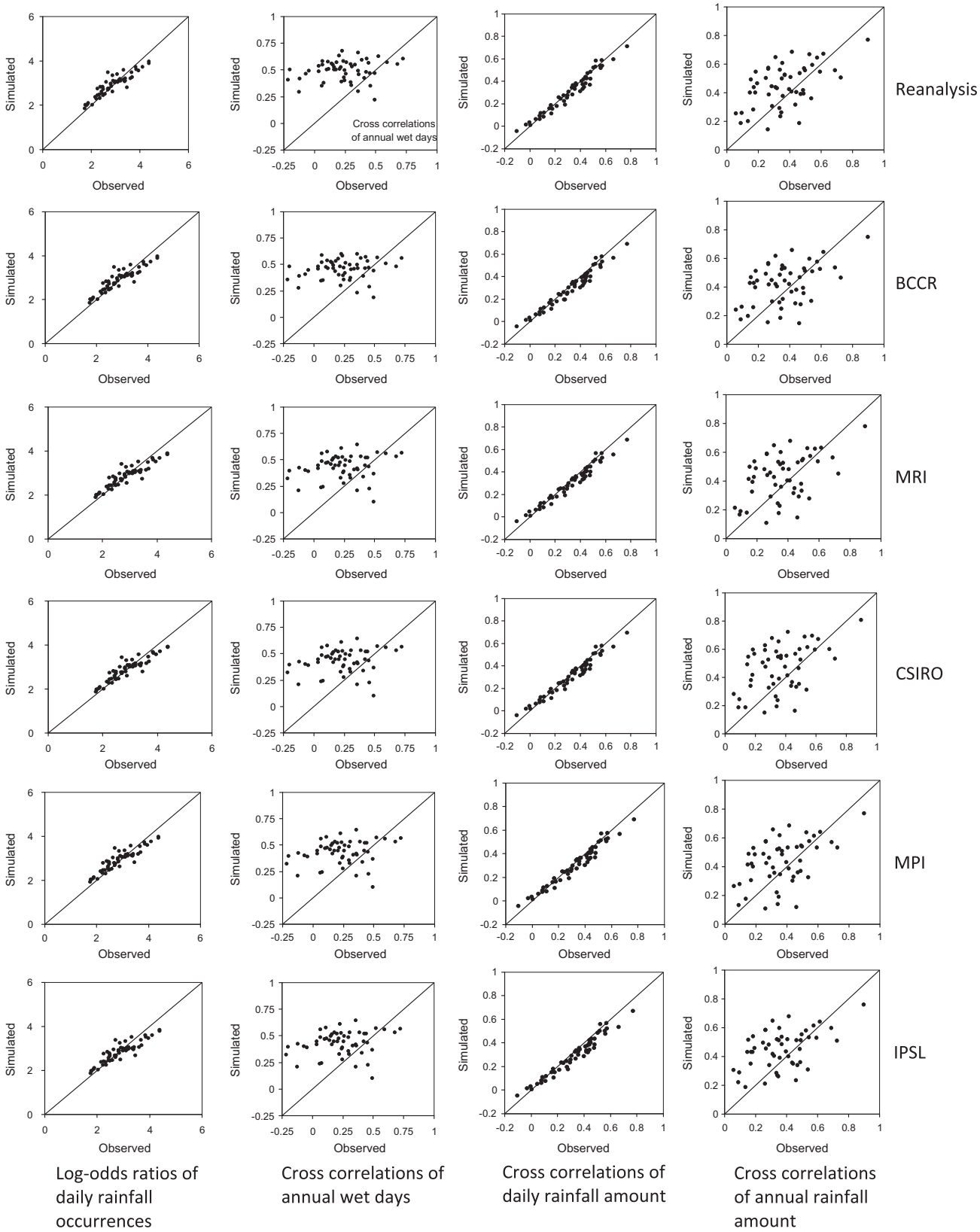

Fig. 6. Observed and modelled log-odds ratios and cross correlations of wet days and rainfall amounts for current climate.

model structure limitations. These results also include a model weighted average estimate. As all the models provide a reasonable estimate of the important observed statistics for the current climate, a simple model weighting procedure is adopted. The procedure evaluates the models on the basis of their performance in reproducing the observed number of wet days, rainfall amount and amount per wet day in a season in the current climate and assigns a weight on the basis of magnitude of sum of squared differ-

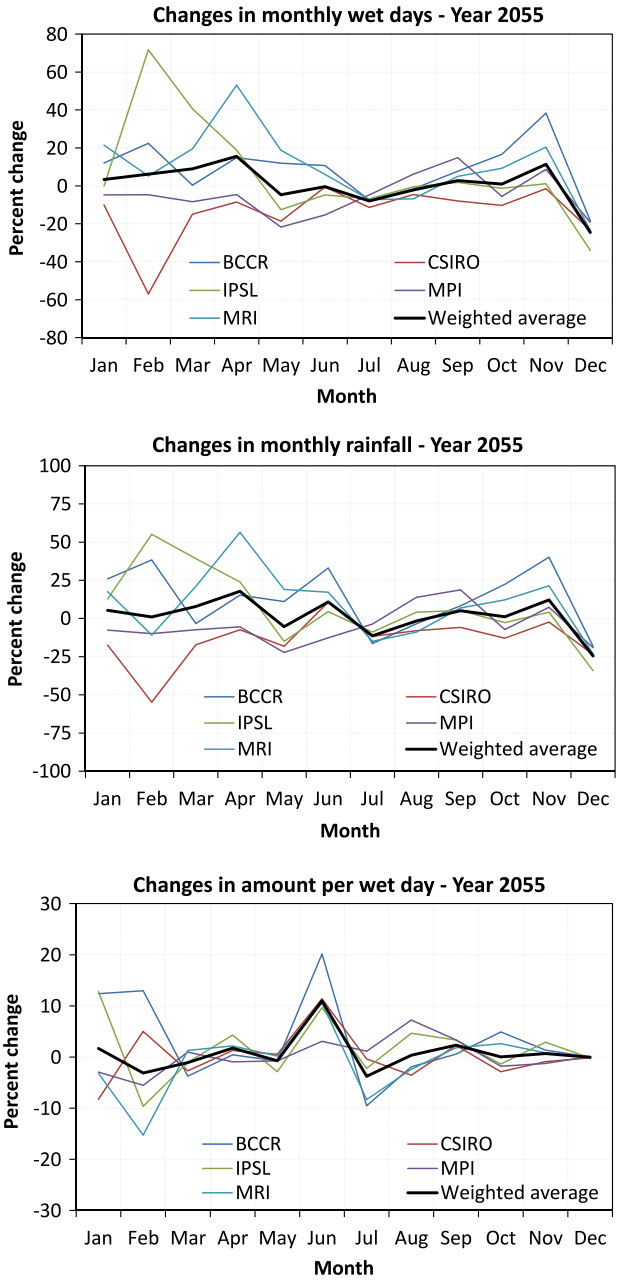

Fig. 7. Projected changes in monthly wet days, rainfall totals and amount per wet day in 2055 (2046–2065).

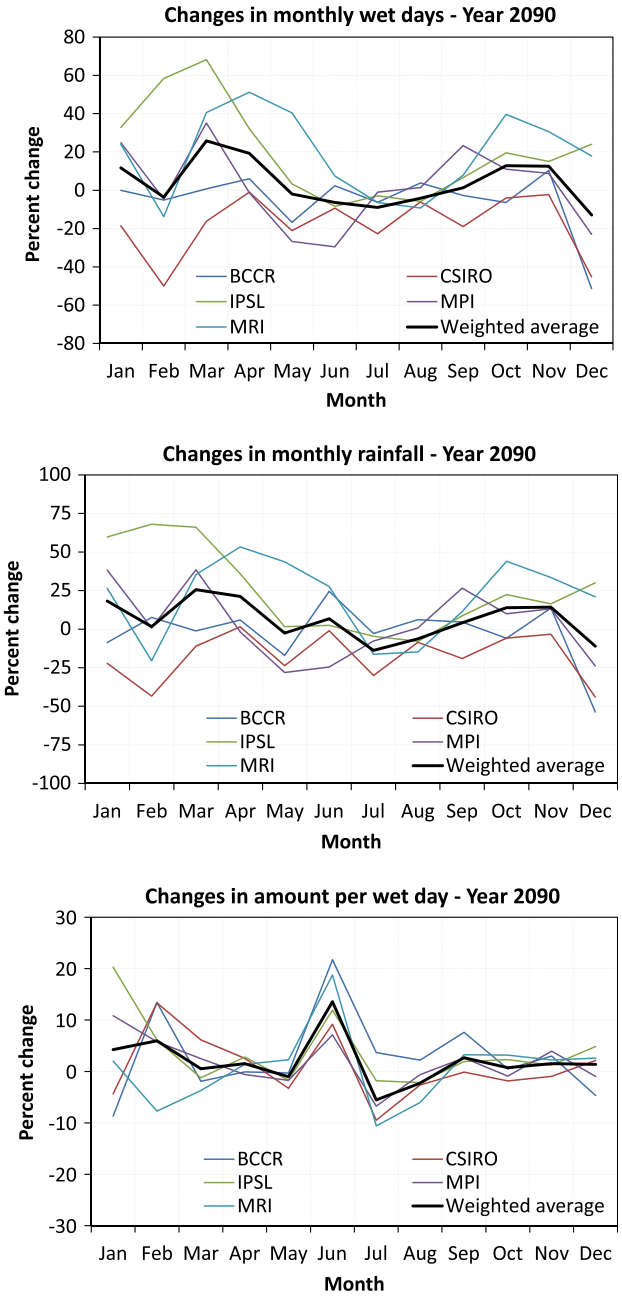

Fig. 8. Projected changes in monthly wet days, rainfall totals and amount per wet day in 2090 (2081–2100).

ences in these statistics. On the basis of this criterion, the models BCCR, CSIRO, IPSL, MPI and MRI are assigned weights as 0.15, 0.25, 0.231, 0.14 and 0.22, respectively.

4.3.1. Area averaged rainfall statistics

Figs. 7 and 8 present the changes in monthly wet days and rainfall amounts in years 2055 and 2090 whereas the percent changes in seasonal and annual number of wet days and rainfall totals are presented in Table 6. By 2055, simulations from all GCMs project no appreciable changes in rainfall in all seasons. Please note that, for non-monsoon seasons (JFMAM and OND) slight variation in number of wet days or rainfall amount may show up as a large percentage change. The projected changes in rainfall are quite consistent across the GCMs for monsoon season. The CSIRO model projects a reduction in number of wet days and rainfall amount in all seasons and months whereas projections from MPI indicate some decreases in pre-monsoon season (first row, Fig. 7 and Table 6). The increases in the number of wet days and rainfall amount during pre-monsoon season by the IPSL model (first and second plots, Fig. 7), although appear large, accounts for differences of less than a day and 2 mm, respectively. Other models project small increases in number of wet days and rainfall amount during non-monsoon seasons. There is no appreciable change in the amount per wet day with all the models projecting heavy rainy days during June (bottom plot, Fig. 7). The models weighted average indicates no appreciable changes in the number of wet days and rainfall amount in year 2055. By 2090, CSIRO predicts appreciable drying in all months with about 15% decrease in monsoon rainfall and wet days (Fig. 8 and Table 6). No changes in seasonal shifts are noticed, however, a weak tendency of the monsoon extending to October is observed (Fig. 8). Considering model averaged statistics,

Table 6
Projected percent changes in seasonal and annual number of wet days and rainfall totals in comparison to GCM current climate.

	Wet days				Rainfall totals			
	JFMAM	JJAS	OND	Annual	JFMAM	JJAS	OND	Annual
Year 2055								
BCCR	12	1	19	4	12	2	23	5
MRI	29	−2	10	2	29	−3	12	1
CSIRO	−16	−6	−9	−8	−15	−5	−11	−6
MPI	−16	−1	−3	−2	−17	1	−5	−1
IPSL	1	−3	−3	−3	0	−1	−3	−1
Weighted average	2	−3	1	−2	2	−2	2	−1
Year 2090								
BCCR	−9	−1	−6	−2	−10	7	−6	5
MRI	43	−2	36	7	45	−2	40	6
CSIRO	−15	−14	−7	−13	−16	−16	−8	−15
MPI	−14	−3	8	−2	−16	−6	8	−5
IPSL	17	−3	19	1	16	−2	22	2
Weighted average	6	−5	11	−2	6	−5	12	−2

Table 7
Projected percent changes in extreme rainfall characteristics in comparison to GCM current climate.

Statistics/model	BCCR	MRI	CSIRO	MPI	IPSL	Weighted average
Year 2055						
Number of dry spells of 2–9 days	6	13	−2	−3	−1	3
Number dry spells of 10–18 days	−2	4	−1	−4	5	1
Number of dry spells of >18 days	−8	−8	1	3	0	−2
Number of wet spells of 2–4 days	4	12	−3	−2	0	2
Number of wet spells of 5–7 days	2	3	−8	−2	1	−1
Number of wet spells of >7 days	4	−6	−8	−5	−6	−5
Average rainfall in wet spells of 2–4 days	2	2	3	1	3	3
Average rainfall in wet spells of 5–7 days	3	3	6	3	7	5
Average rainfall in wet spells of >7 days	2	−4	0	4	−1	0
Number of days with heavy rainfall	6	1	−6	−1	−1	−1
Year 2090						
Number of dry spells of 2–9 days	−1	22	−2	0	8	6
Number dry spells of 10–18 days	0	2	6	−4	6	3
Number of dry spells of >18 days	−4	−11	1	4	3	−1
Number of wet spells of 2–4 days	−4	20	−3	1	9	5
Number of wet spells of 5–7 days	−9	12	−10	−1	8	0
Number of wet spells of >7 days	0	−3	−19	−7	−6	−8
Average rainfall in wet spells of 2–4 days	5	5	5	2	5	4
Average rainfall in wet spells of 5–7 days	11	8	7	2	8	7
Average rainfall in wet spells of >7 days	10	−6	−11	−7	−6	−5
Number of days with heavy rainfall	4	7	−15	−6	2	−2

no appreciable changes at annual level in year 2090 are noted with minor increases in the number of wet days and rainfall amount during pre- and post-monsoon seasons. Similar to year 2055, the amount per wet day is projected to increase by about 10% during June.

Percent changes in average number of wet and dry spells of varying durations, associated rainfall in wet spells and number of days with heavy rainfall (3rd percentile of daily rainfall) in years 2055 and 2090 are also evaluated and reported in Table 7. Some variations from model to model are noted with averages indicating no appreciable changes in these statistics. Occurrences of shorter duration wet spells (up to 7 days) may increase in future with associated increase in rainfall amount. Wet spells of longer durations may decrease in future. However, these changes are not significant. Number of days with heavy rainfall does not show any appreciable changes.

The rainfall changes discussed here are derived using averages over the study area. It would be of interest to examine whether there are spatial variations in rainfall patterns or frequency of rainfall extremes is changing in the future. These aspects are examined in the following sub-section.

4.3.2. Changes at individual stations

Figs. 9 and 10 present the percent changes in annual number of wet days, annual rainfall amount and per wet day rainfall in a year at individual station in years 2055 and 2090. In these plots changes at individual station locations are marked as circles with hollow indicating a decrease and filled one suggesting an increase in the statistic shown. A reference circle size for a 10% change is also included. No appreciable changes in rainfall across stations and GCMs are noted. CSIRO downscaled simulations project a spatially consistent decrease of around 7% in year 2055 and 15% in year 2090 at all stations. BCCR and MRI project nominal increases in annual number of wet days and rainfall amount at majority of stations.

We also examined the changes in year-to-year distribution of annual wet days, rainfall and maximum daily rainfall and noted no major changes (results not included). It may be noted here that

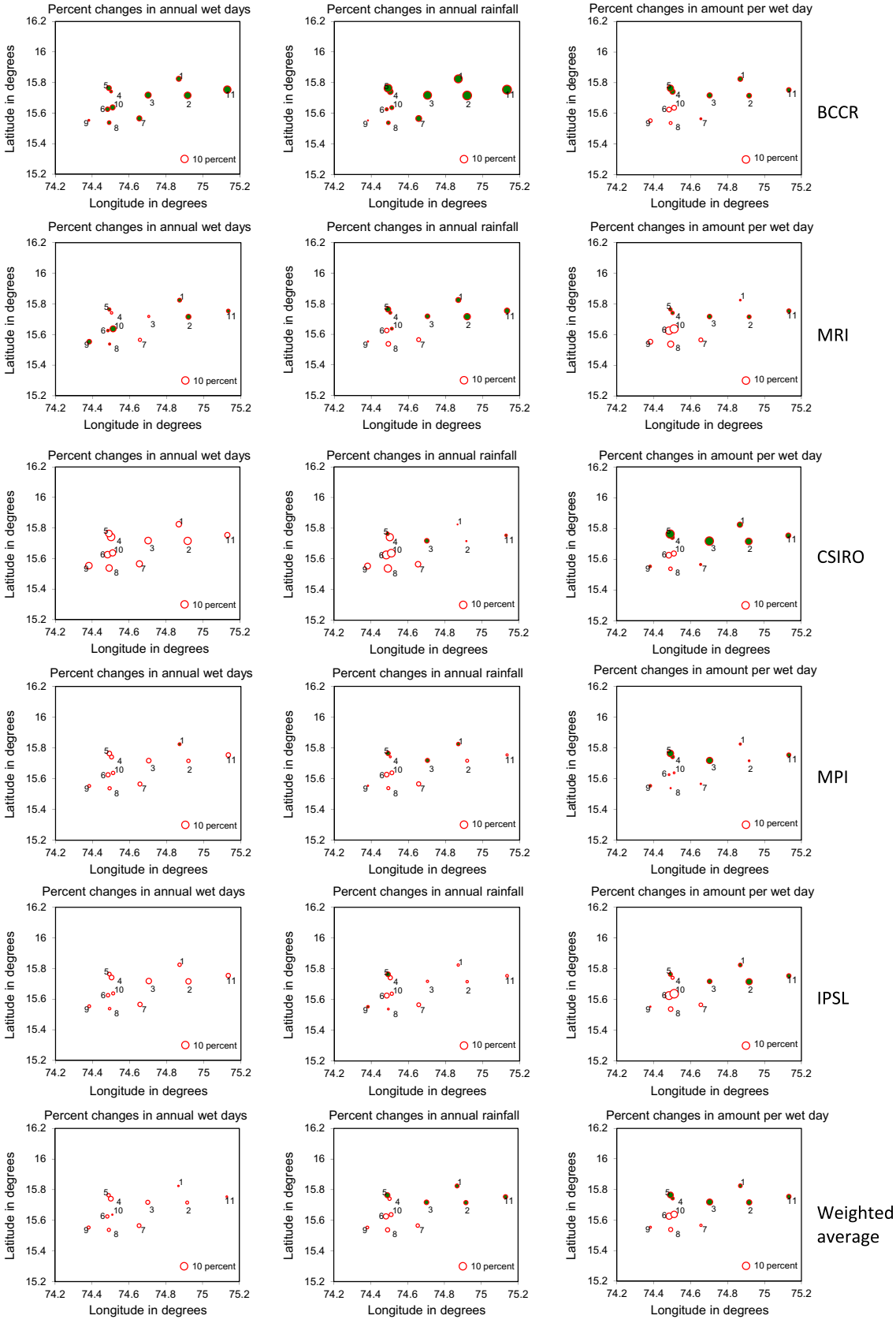

Fig. 9. Changes in annual wet days and rainfall totals at individual stations in 2055 (2046–2065) in comparison to the current climate. Hollow circles indicate a decrease while filled one an increase.

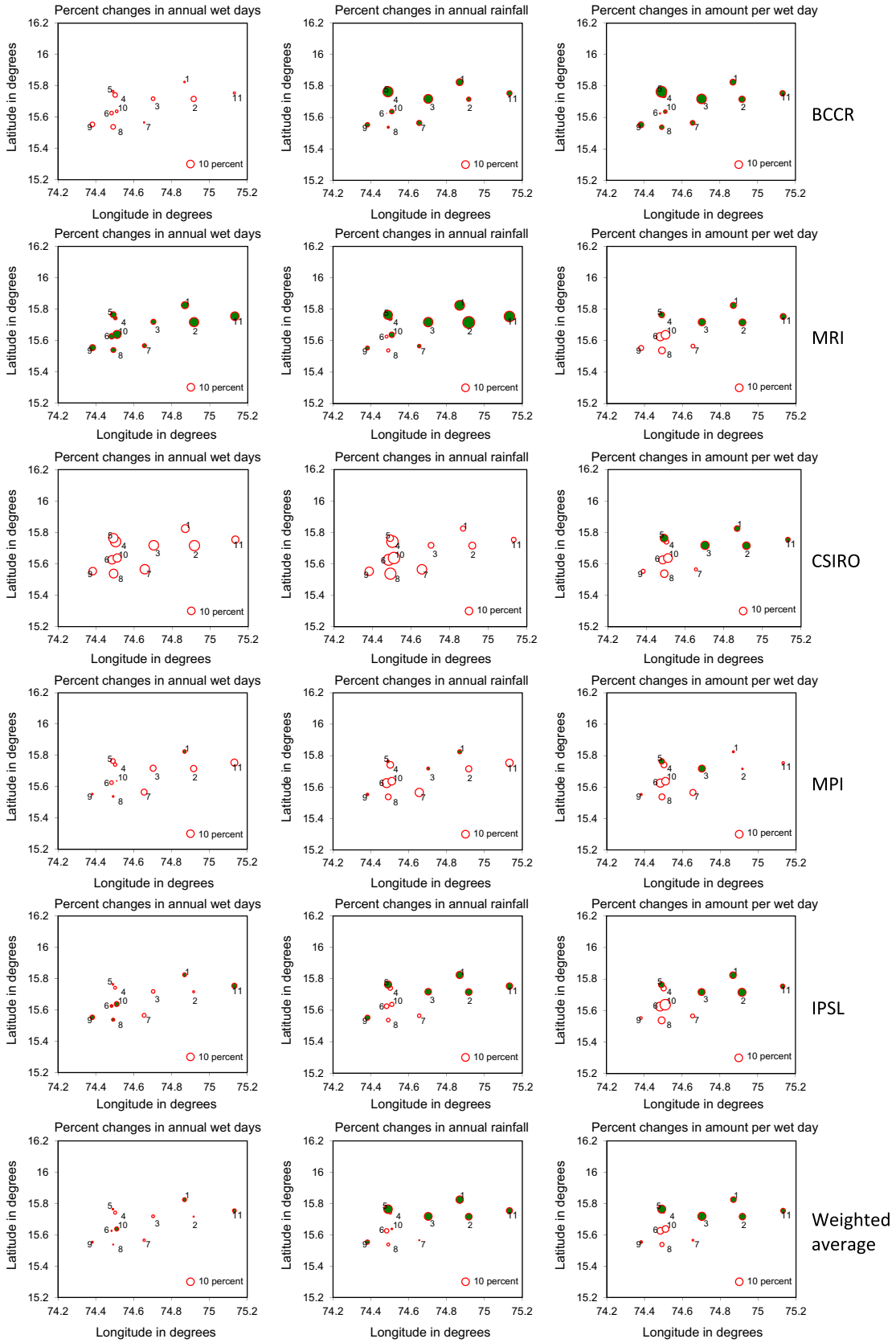

Fig. 10. Changes in annual wet days and rainfall totals at individual stations in 2090 (2081–2100) in comparison to the current climate. Hollow circles indicate a decrease while filled one an increase.

the results drawn hare are based on single ensemble of five GCMs and addition or omission of one or more GCM and ensembles may change the predictions.

5. Summary and conclusions

This paper has demonstrated the applicability of a stochastic downscaling framework for simulation of multi-site rainfall in future climate settings. The coarse spatial resolution of GCMs (~300 km) provides only a limited representation of the realistic topographical features like the Western Ghats (along the west coast of India) in the model structure and consequently fails to reproduce their predominant influence on the regional rainfall patterns (Krishna Kumar et al., 2011). The downscaling approaches, similar to the one used in the study, allow to consider these influences on the simulated rainfall.

Downscaling models like MMM-KDE used in this application, are capable of simulating rainfall at a network of stations whilst maintaining the spatial dependence attributes and therefore best suited for use in catchment management practice, where the nature of spatial variations in rainfall has important influences on the streamflows and flooding. Also, important temporal attributes of rainfall like distribution of wet and dry spells, number of wet days and rainfall amounts at individual stations have significant impacts in crop simulation studies and drought management applications. Such spatio-temporal rainfall attributes assume even more importance when the downscaling procedure is applied for investigating possible changes that might be experienced by hydrological, agricultural and ecological systems in future climates.

The comparison of standard rainfall attributes such as the number of wet days, average rainfall amounts, maximum daily rainfall amount, wet and dry spells and other diagnostics indicate that downscaled results of MMM-KDE model agree fairly well with the observed record for the current climate. Rainfall simulations over the study region for years 2055 and 2090 using projections of five different GCMs indicate CSIRO to be a fairly dry model in comparison to the other GCMs used in the study. Combined results of all GCMs indicate slight decrease in monsoon rainfall over the study region however, it is not statistically significant. Additionally, the results of investigations carried out on extreme related statistics and spatial rainfall distribution indicate no significant changes in these rainfall attributes.

While none of the downscaling studies mentioned in the introduction have focused over the study area, an interpretation of their results over the study region may provide some insight into the likely changes that are expected in a warmer climate. Krishna Kumar et al. (2011) examined the changes in the summer monsoon over India corresponding to the IPCC-SRES A1B emission scenarios using three simulations from Hadley Center Coupled Model and projected −20% to +20% changes in the monsoon rainfall by the year 2080 over the study region across the three simulations. Similarly, results of Turner and Slingo (2009) indicated −1 to +1 mm/day changes in the mean rainfall in the future over the study region. Rajendran and Kitoh (2008) used a global super high-resolution GCM with a spatial grid size of about 20 km over India. Their results suggested a decrease of 2 mm/day in the monsoon rainfall over the catchment by 2080. The outcomes of these studies are largely dependent on the selection of a GCM and scenario and show no conclusive pattern of the likely changes in the rainfall in the future over the study area.

A significant issue in downscaling applications relates to the incorporation of uncertainty in the climate projections as simulated by different GCMs. This uncertainty is typically included by considering an ensemble of models, with an important example being the Coupled Model Intercomparison Project phase 3 (CMIP3) of GCMs (Meehl et al., 2007). Even very recently, many studies have only used a single GCM output (Austin et al., 2010; Mehrotra and Sharma, 2010; Holman et al., 2009; Mileham et al., 2009; Toews and Allen, 2009; van Roosmalen et al., 2009). Findings of a recent study suggest that the greatest source of the uncertainty in the downscaled results comes from the differences in the climate projections (Crosbie et al., 2011). The use of climate projections from multiple GCMs in the study has enabled to incorporate the uncertainty in the downscaled rainfall results that arises through the use of single GCM. Although, the selection of GCMs is influenced by the availability of atmospheric variables at daily time scale at the CMEP3 archive, the selected five GCMs are expected to explain a major part of the variability across GCMs. In a recent study, Ojha et al. (in press) assessed the performance of 17 GCMs using the CMIP3 data and assigned a ranking to these models on the basis of their ability in reproducing the monthly and annual rainfall statistics over India. On the basis of this ranking criterion, the models used in the study are ranked as 2, 5, 6, 10 and 13. Although, not a robust measure, these rankings cover a broad range and suggest that the models used in the study roughly cover the GCMs uncertainty spectrum.

Acknowledgements

This research is supported by the Australia India Strategic Research Fund (AISRF-ST030111). We acknowledge the modeling groups, the Program for Climate Model Diagnosis and Intercomparison (PCMDI) and the WCRP's Working Group on Coupled Modelling (WGCM) for their roles in making available the WCRP CMIP3 multi-model dataset. Support of this dataset is provided by the Office of Science, US Department of Energy.

References

Anandhi, A., Srinivas, V.V., Nanjundiah, Ravi S., Nagesh Kumar, D., 2008. Downscaling precipitation to river basin in India for IPCC SRES scenarios using support vector machine. Int. J. Climatol. 28, 401–420.

Ashrit, R., Douville, H., Kumar, K.K., 2003. Response of the Indian monsoon and ENSO-monsoon teleconnection to enhanced greenhouse effect in the CNRM coupled model. J. Meteorol. Soc. Jpn. 81, 779–803. http://dx.doi.org/10.2151/jmsj.81.779.

Austin, J., Zhang, L., Jones, R., Durack, P., Dawes, W., Hairsine, P., 2010. Climate change impact on water and salt balances: an assessment of the impact of climate change on catchment salt and water balances in the Murray-Darling Basin, Australia. Clim. Change 100 (3–4), 607–631. http://dx.doi.org/10.1007/s10584-009-9714-z.

Buishand, T.A., Shabalova, M.V., Brandsma, T., 2004. On the choice of the temporal aggregation level for statistical downscaling of precipitation. J. Clim. 17 (9), 1816–1827.

Cavazos, T., 1999. Large-scale circulation anomalies conducive to extreme precipitation events and derivation of daily rainfall in Northeastern Mexico and Southeastern Texas. J. Clim. 12, 1506–1523.

Charles, S.P., Bates, B.C., Hughes, J.P., 1999. A spatio-temporal model for downscaling precipitation occurrence and amounts. J. Geophys. Res. 104 (D24), 31657–31669.

Charles, S.P., Bates, B.C., Smith, I.N., Hughes, J.P., 2004. Statistical downscaling of daily precipitation from observed and modelled atmospheric fields. Hydrol. Process. 18, 1373–1394.

Crane, R.G., Hewitson, B.C., 1998. Doubled CO_2 precipitation changes for the Susquehanna Basin: down-scaling from the GENESIS general circulation model. Int. J. Climatol. 18, 65–76.

Crosbie, R.S., Dawes, W.R., Charles, S.P., Mpelasoka, F.S., Aryal, S., Barron, O., Summerell, G.K., 2011. Differences in future recharge estimates due to GCMs, downscaling methods and hydrological models. Geophys. Res. Lett. 38, L11406. http://dx.doi.org/10.1029/2011GL047657.

Easterling, D., 1999. Development of regional climate change scenarios using a downscaling approach. Clim. Change 41, 615–634.

Edwards, A.W.F., 1963. The measure of association in a 2 × 2 table. J. R. Stat. Soc. A 126 (1), 109–114.

Evans, J.P., Ronald, B.S., Robert, J.O., 2004. Middle east climate simulation and dominant precipitation processes. Int. J. Climatol. 24, 1671–1694.

Fordham, D.A., Wigley, T.M.L., Watts, M.J., Brook, B.W., 2012. Strengthening forecasts of climate change impacts with multi-model ensemble averaged

projections using MAGICC/SCENGEN 5.3. Ecography 35, 4–8. http://dx.doi.org/10.1111/j.1600-0587.2011.07398.
Frost, A.J., Charles, S.P., Timbal, B., Chiew, F.H.S., Mehrotra, R., Nguyen, K.C., Chandler, R.E., McGregor, J.L., Fu, G., Kirono, D.G.C., Fernandez, E., Kent, D.M., 2011. A comparison of multisite daily rainfall downscaling techniques under Australian conditions. J. Hydrol. 408 (12). http://dx.doi.org/10.1016/j.jhydrol.2011.06.021.
Gadgil, S., Abrol, Y.P., Rao, S., 1999. On growth and fluctuation of Indian food grain production. Curr. Sci. 76, 548–556.
Gadgil, S., Gadgil, S., 2006. The Indian monsoon, GDP and agriculture. Econ. Polit. Wkly 11, 4887–4895.
Harpham, C., Wilby, R.L., 2005. Multi-site downscaling of heavy daily precipitation occurrence and amounts. J. Hydrol. 312, 1–21.
Harrold, T.I., Sharma, A., Sheather, S.J., 2003. A nonparametric model for stochastic generation of daily rainfall occurrence. Water Resour. Res. 39 (12), 1343. http://dx.doi.org/10.1029/2003WR002570.
Hewitson, B.C., Crane, R.G., 1996. Climate downscaling: techniques and application. Clim. Res. 7, 85–95.
Holman, I.P., Tascone, D., Hess, T.M., 2009. A comparison of stochastic and deterministic downscaling methods for modelling potential groundwater recharge under climate change in East Anglia, UK: implications for groundwater resource management. Hydrogeol. J. 17 (7), 1629–1641. http://dx.doi.org/10.1007/s10040-009-0457-8.
Hu, Z.Z., Latif, M., Roeckner, E., Bengtsson, L., 2000. Intensified Asian summer monsoon and its variability in a coupled model forced by increasing greenhouse gas concentrations. Geophys. Res. Lett. 27, 2618–2684. http://dx.doi.org/10.1029/2000GL011550.
Hughes, J.P., Guttorp, P., Charles, S.P., 1999. A non-homogeneous hidden Markov model for precipitation occurrence. Appl. Stat. 48 (1), 15–30.
IPCC, 2007. Climate change 2007: the physical science basis. In: Solomon, S., Qin, D., Manning, M., Chen, Z., Marquis, M., Averyt, K.B., Tignor, M., Miller, H.L. (Eds.), Contribution of Working Group I to the Fourth Assessment Report of the Intergovernmental Panel on Climate Change. Cambridge University Press, Cambridge, United Kingdom and New York, NY, USA, 996 pp.
Johnson, F., Sharma, A., 2011. Accounting for interannual variability: a comparison of options for water resources climate change impact assessments. Water Resour. Res. 47 (4).
Johnson, F., Sharma, A., 2012. A nesting model for bias correction of variability at multiple time scales in general circulation model precipitation simulations. Water Resour. Res. 48, W01504. http://dx.doi.org/10.1029/2011WR010464.
Krishna Kumar, K., Patwardhan, S.K., Koteswara Rao, K., Jones, R., 2011. Simulated projections for summer monsoon climate over India by a high-resolution regional climate model (PRECIS). Curr. Sci. 101 (3), 312–326.
May, W., 2002. Simulated changes of the Indian summer monsoon under enhanced greenhouse gas conditions in a global time-slice experiment. Geophys. Res. Lett. 29, 1118.
Meehl, G.A., Arblaster, J.M., 2003. Mechanisms for projected future changes in South Asian monsoon precipitation. Clim. Dynam. 21, 659–675.
Meehl, G., Stocker, T., Collins, W., Friedlingstein, P., Gaye, A., Gregory, J., Kitoh, A., Knutti, R., Murphy, J., Noda, A., Raper, S., Watterson, I., Weaver, A., Zhao, Z.-C., 2007. Climate Change 2007: The Physical Science Basis. Working Group I to the Fourth Assessment Report of the Intergovernmental Panel on Climate Change.
Meehl, G.A., Arblaster, J.M., Collins, W.D., 2008. Effects of black carbon aerosols on the Indian monsoon. J. Clim. 21, 2869–2882.
Mehrotra, R., Sharma, A., 2005. A nonparametric nonhomogeneous hidden Markov model for downscaling of multi-site daily rainfall occurrences. J. Geophys. Res. 110, D16108. http://dx.doi.org/10.1029/2004JD005677.
Mehrotra, R., Srikanthan, R., Sharma, A., 2006. A comparison of three stochastic multi-site precipitation occurrence generators. J. Hydrol. 331, 280–292. http://dx.doi.org/10.1016/j.jhydrol.2006.05.016.
Mehrotra, R., Sharma, A., 2007a. A semi-parametric model for stochastic generation of multi-site daily rainfall exhibiting low frequency variability. J. Hydrol. 335, 180–193. http://dx.doi.org/10.1016/j.jhydrol.2006.11.011.
Mehrotra, R., Sharma, A., 2007b. Preserving low-frequency variability in generated daily rainfall sequences. J. Hydrol. 345, 102–120. http://dx.doi.org/10.1016/j.jhydrol.2007.08.003.
Mehrotra, R., Sharma, A., 2010. Development and application of a multisite rainfall stochastic downscaling framework for climate change impact assessment. Water Resour. Res. 46 (W07526), 17. http://dx.doi.org/10.1029/2009WR008423.
Mileham, L., Taylor, R.G., Todd, M., Tindimugaya, C., Thompson, J., 2009. The impact of climate change on groundwater recharge and runoff in a humid, equatorial catchment: sensitivity of projections to rainfall intensity. Hydrol. Sci. J. 54 (4), 727–738. http://dx.doi.org/10.1623/hysj.54.4.727.
Ojha, R., Nagesh Kumar, D., Sharma, A., Mehrotra, R., 2012. Assessing severe drought and wet events over India in a future climate using nested bias correction approach. J. Hydrol. Eng., Am. Soc. Civ. Eng. (ASCE). http://dx.doi.org/10.1061/(ASCE)HE.1943-5584.0000585.
Pierce, D.W., Barnett, T.P., Santer, B.D., Gleckler, P.J., 2009. Selecting global climate models for regional climate change studies. Proc. Natl. Acad. Sci. USA 106, 8441–8446.
Rajendran, K., Kitoh, A., 2008. Indian summer monsoon in future climate projection by a super high-resolution global model. Curr. Sci. 95 (11), 1560–1569.
Scott, D.W., 1992. Multivariate Density Estimation: Theory, Practice and Visualization. John Wiley, New York.
Sharma, A., O'Neill, R., 2002. A nonparametric approach for representing interannual dependence in monthly streamflow sequences. Water Resour. Res. 38 (7), 5.1–5.10.
Sharma, A., Mehrotra, R., Johnson, F., in press. A new framework for modelling future hydrologic extremes: nested bias correction as a precursor to stochastic rainfall downscaling. In: Surampalli, Rao Y., Ojha, C.S.P. (Eds.), Green House Gas Emissions and Climate Change. American Society of Civil Engineers (ASCE), USA.
Solomon, S., Qin, D., Manning, M., et al., 2007. "Technical summary" in climate change 2007: physical science basis. In: Solomon, S., Qin, D., Manning, M., Chen, Z., Marquis, M., Averyt, K.B., Tignor, M., Miller, H.L. (Eds.), Contribution of Working Group I to the Fourth Assessment Report of the Intergovernmental Panel on Climate Change. Cambridge University Press, Cambridge, United Kingdom and New York, NY, USA.
Stehlík, J., Bárdossy, A., 2002. Multivariate stochastic downscaling model for generating daily precipitation series based on atmospheric circulation. J. Hydrol. 256, 120.
Stephenson, D.B., Douville, H., Rupa Kumar, K., 2001. Searching for a fingerprint of global warming in the Asian summer monsoon. Mausam 52, 213–220.
Toews, M.W., Allen, D.M., 2009. Simulated response of groundwater to predicted recharge in a semi-arid region using a scenario of modeled climate change. Environ. Res. Lett. 4 (3), 035003. http://dx.doi.org/10.1088/1748- 9326/4/3/035003.
Trenberth, K.E., Dai, A., Rasmussen, R.M., Parsons, D.B., 2003. The changing character of precipitation. Bull. Am. Meteorol. Soc. 2003 (September), 1205–1217. http://dx.doi.org/10.1175/BAMS-84-9-1205.
Turner, A.G., Inness, P.M., Slingo, J.M., 2007. The effect of doubled CO_2 and model basic state biases on the monsoon-ENSO system. I: mean response and interannual variability. Q. J. R. Meteorol. Soc. 133, 1143–1157. http://dx.doi.org/10.1002/qj.82.
Turner, A.G., Slingo, J.M., 2009. Uncertainties in future projections of extreme precipitation in the Indian monsoon region. Atmos. Sci. Lett. 10(3), 152–158. http://dx.doi.org/10.1002/asl.223. ISSN 1530–261X.
van Roosmalen, L., Sonnenborg, T.O., Jensen, K.H., 2009. Impact of climate and land use change on the hydrology of a large-scale agricultural catchment. Water Resour. Res. 45, W00A15. http://dx.doi.org/10.1029/2007WR006760.
Vrac, M., Naveau, P., 2007. Stochastic downscaling of precipitation: from dry to heavy rainfalls. Water Resour. Res. 43, W07402. http://dx.doi.org/10.1029/2006WR005308.
Wilby, R.L., Wigley, T.M.L., 1997. Downscaling general circulation model output: a review of methods and limitations. Prog. Phys. Geogr. 21, 530–548.
Wilks, D.S., 1998. Multisite generalization of a daily stochastic precipitation generation model. J. Hydrol. 210, 178–191.